JOC The Journal of Organic Chemistry

Note

pubs.acs.org/joc

Unraveling the Role of Alkyl F on CH−π Interactions and Uncovering the Tipping Point for Fluorophobicity

Mark R. Ams,*[,†] Michael Fields,[†,∥] Timothy Grabnic,[†,∥] Benjamin G. Janesko,[‡] Matthias Zeller,[§] Rose Sheridan,[†,∥] and Amanda Shay[†,∥]

[†]Department of Chemistry, Allegheny College, 520 North Main Street, Meadville, Pennsylvania 16335-3902, United States

[‡]Department of Chemistry, Texas Christian University, 2800 Souh University Drive, Fort Worth, Texas 76109, United States

[§]Department of Chemistry, Youngstown State University, One University Plaza, Youngstown, Ohio 44555, United States

Supporting Information

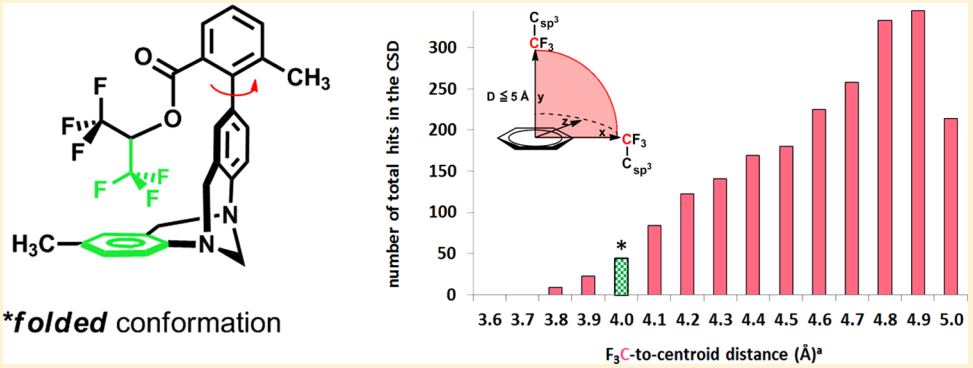

ABSTRACT: Although fluorine often plays an influential role in molecular recognition, little is known about the effect of aliphatic fluorine on the CH−π interaction in solution. A series of molecular balances were synthesized that contain fluorinated and nonfluorinated alkyl groups. Our findings indicate that fluorine's polarizing ability does enhance CH−π binding and depends on molecular orientation. Surprisingly, when the terminal end of the alkyl group is completely fluorinated, the balance tips toward fluorophobicity and assumes an unusual constrained conformation.

The ability to correctly predict the interactions occurring among molecules in solution without engaging in laboratory experimentation is an unrealized goal in modern chemistry, in part due to the enormous challenge of properly accounting for the many forces that act upon molecules in dynamic systems. Ideally, the behavior of complicated processes such as protein folding and drug−receptor binding is predicted by applying the proper algorithms derived from experimental data.[1] Current computational approaches, however, are limited by the lack of experimental data derived from the forces that drive these processes. One of the specific information gaps that contributes to the inaccuracy of current algorithms is the experimentally elusive data occurring in noncovalent interactions.[2] Among the weakest of these interactions is the CH−π interaction, which is worth just under 1 kcal/mol in energy but is often very influential in molecular recognition.[3]

While some basic principles of the CH−π interaction are now understood,[4] the rapid emergence of fluorine (F) in the past decade as a structural design feature to facilitate binding has uncovered a largely unexplored area in which these two entities intersect. Fluorine is now represented in at least 20% of drugs on the market today[5] and is increasingly engineered into the design of oligopeptides,[6] proteins,[7] and small-molecule inhibitors.[8] Many of these involve fluorine atoms directly attached to aromatics,[9,10] systems that have been thoroughly studied.[11] However, much less is known about how sp^3-centered aliphatic fluorine influences CH−π attraction. Few studies report solution-phase experimental free energies for aliphatic fluorine interacting with electron-rich π systems like those of aromatic amino acids.[12,13] Many important drugs contain aliphatic fluorine,[14] while many more are being intensely sought after by synthetic chemists,[15] underscoring the need for accurate predictive binding models. This is emphasized by Ho,[1] Zhu,[16] and others,[17] who argue that such data is needed to validate QM and MM calculations as well as to treat molecular modeling issues involving halogens.

We employed the Wilcox molecular torsion balance[18] as a precise tool to systematically quantify the relative Gibbs free energies of fluorinated alkyl groups attracted to π systems. As with related balances that measure nonbonding interaction strengths,[19] the Wilcox balance scaffold is structurally designed to measure the CH−π attraction by using two separated conformational states (folded and unfolded, Figure 1) that are both directly observable and quantifiable by NMR spectroscopy at ambient temperature. In the folded conformation, the R

Received: May 13, 2015
Published: July 8, 2015

DOI: 10.1021/acs.joc.5b01072
J. Org. Chem. 2015, 80, 7764−7769

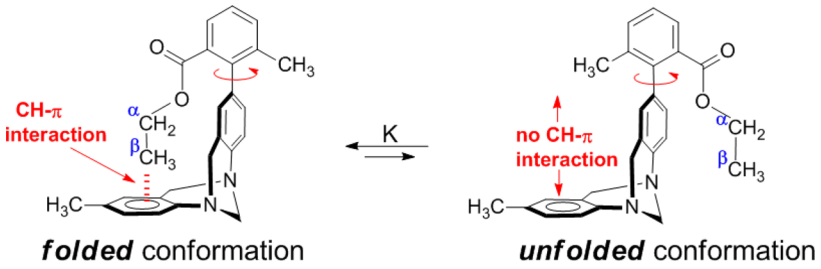

Figure 1. Folded and unfolded conformational states of molecular balance **2** (R = $^{\alpha}CH_2{}^{\beta}CH_3$) highlighting the β-carbon CH−π interaction. The barrier to rotation (red arrow) is approximately 16 kcal/mol,[18a] allowing each isomer to be observable and quantified by ^{1}H NMR.

group is situated directly above the bottom π shelf and is subject to CH− attractions. Any such attractions between R and the vertical aromatic ring are canceled due to an equivalent one in the unfolded state, thereby isolating those occurring with the bottom shelf. R groups of interest can be easily tailored during synthesis, allowing us to survey aliphatic R groups containing fluorine atoms.

To study the influence of fluorine systematically, balances **1**−**8** containing aliphatic R groups with varying amounts of fluorine were synthesized and characterized by X-ray crystallography, and their folded/unfolded ratios were determined by ^{1}H NMR spectroscopy in $CDCl_3$ solvent (Table 1).[20] Compound **1**, in which R = methyl, was used as our control model given its low preference for either conformation. Lengthening the aliphatic chain with one carbon and transforming it to an ethyl group as shown in balance **2** permits it to participate in the CH−π attraction. This lengthening yields an experimental folding energy (ΔG°_{fold}) of −0.35 kcal/mol.

Table 1. Folding of Balances 1−8

balance	R	K (folded/unfolded)[a]	ΔG°_{fold}[b] (kcal/mol)
1	$^{\alpha}CH_3$	1.07	−0.04
2	$^{\alpha}CH_2{}^{\beta}CH_3$	1.79	−0.35
3	$^{\alpha}CH_2{}^{\beta}CH_2F$	2.01	−0.41
4	$^{\alpha}CH_2{}^{\beta}CHF_2$	2.00	−0.41
5	$^{\alpha}CH_2{}^{\beta}CF_3$	1.48	−0.23
6	$^{\alpha}CH(^{\beta}CH_3)_2$	2.09	−0.44
7	$^{\alpha}CH(^{\beta}CH_2F)_2$	2.35	−0.50
8	$^{\alpha}CH(^{\beta}CF_3)_2$	1.19	−0.10

[a]Ratio of solute as determined by NMR spectroscopy in $CDCl_3$ at 298 K. [b]The uncertainty in ^{1}H NMR integration measurements has an estimated error value of ±0.02 kcal/mol.

Reasoning that iterative substitution of Hs for fluorines on the β-carbon would polarize the remaining hydrogens and render them more acidic toward the bottom π shelf,[21] we searched for possible enhanced folding preferences for balances **3** and **4** and their isopropyl counterparts **6** and **7**. However, the fluorine substitutions had an overall modest effect on the experimental folding ratios. Close examination of the X-ray crystal structures of balances **2**−**4**, **6**, and **7** in their folded conformations show that the expected CH−π binding mode still operates and that the C−F bond(s) point away from the π shelf. The optimal CH−π binding orientation for these alkyl groups, where the H points orthogonally toward the aromatic ring,[22] is not achievable within the torsion balance framework and results in only small net changes in folding when R is fluorinated (Figure 2).[23]

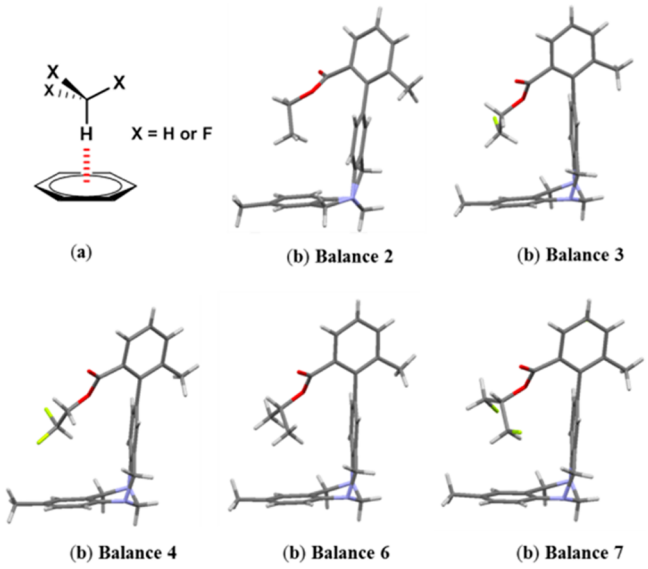

Figure 2. (a) Optimal orthogonal binding orientation for CHX_3 with benzene.[22] (b) X-ray crystal structures of balances **2**−**4**, **6** and **7** in the folded conformation. Balance **5** did not crystallize. Disorder in crystals **2** and **4** is omitted with only the major moieties shown (95.5(4)% occupancy in **2**, 0.761(3) occupancy in **4**). See the Supporting Information for details.

The most surprising result from the series is that complete fluorination of the β-carbon still results in folding. The ΔG°_{fold} for the trifluoromethyl derivatives **5** and **8** were −0.23 and −0.10 kcal/mol, respectively. Since aliphatic fluorine repels π clouds in solution,[24] we therefore anticipated that **5** and **8** would either strongly disfavor folding or be forced to invoke a longer range (and thus only weakly attractive) CH−π effect from the α-carbon. However, the X-ray crystal structure of **8** (Figure 3) shows its electron-deficient β-carbon positioned ∼5° from the center of the π shelf at a distance of 3.968 Å.

Closer inspection of the X-ray structure of balance **8** shows that the $-CF_3$ carbon atom hovers directly above the center of the π shelf, where π-density is at its lowest, and that the polarized C−F bonds of that group point themselves toward the positively polarized benzenoid rim. One explanation for this arrangement is the existence of a direct electrostatic attraction between these polarized groups, similar to that described by Wheeler and Houk (for substituted benzene with benzene[25]). Using dispersion-corrected density functional theory (DFT-D) in continuum chloroform, we sought to capture this apparent switch in binding modes for **5** and **8** as compared to the CH−π attraction occurring in **2**−**4**, **6**, and **7**. The calculations, which focused on obtaining the folding energies ΔE_{fold} of balances **1**−**8** and on isolated benzene−CH_nF_{4-n} complexes (for reference),

DOI: 10.1021/acs.joc.5b01072
J. Org. Chem. 2015, 80, 7764−7769

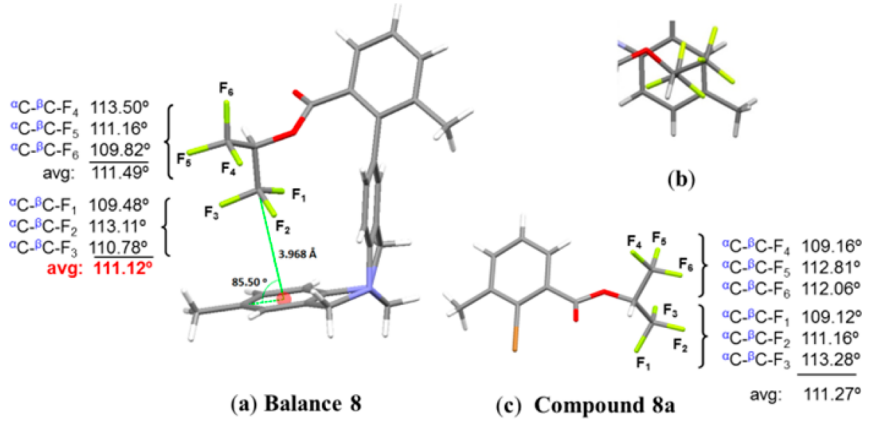

Figure 3. X-ray crystal structures and highlighted geometries. (a) Balance **8**. (b) X-ray fragment of balance **8** (top-down view) showing the CF_3–π orientation. (c) Hexafluoro ester **8a**. Inspection of the crystal lattices in each shows that there are no close intermolecular CF_3–π contacts.

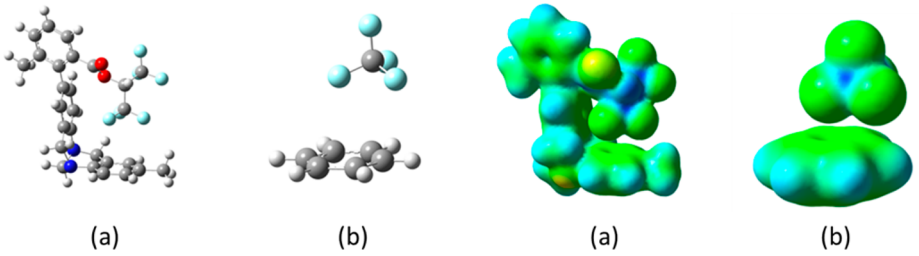

Figure 4. Gas-phase ωB97X-D/6-31G(d) DFT computed geometries and molecular density isosurfaces (0.01 electrons/Bohr^3) colored by molecular electrostatic potential. (a) Balance **8**. (b) CF_4–benzene complex. Surfaces are colored from electrostatic potential −0.15 au (green) to +0.15 au (blue).

roughly correlate with the observed $\Delta G°_{fold}$'s and do capture an electrostatic attraction for **8** (see the Supporting Information).[22,26] Figure 4 shows the anticipated regions of negative charge density on the fluorines and that the electropositive $-CF_3$ carbon prefers to hover above an electron-rich benzene carbon below it, much like a CF_4–benzene complex does. The computed ΔE_{fold} for **8**, however, is less negative than it is for the typical CH–π interaction in **2** (−1.99 vs −2.16 kcal/mol in chloroform). Calculations on balance **5** predict that the CF_3–π interaction competes weakly with an $^{\alpha}$CH–π attraction (−2.7 versus −1.8 kcal/mol, suggesting that 22% of **5** would have the $^{\alpha}$CH–π interaction at room temperature); this is stronger than a typical nonhalogenated CH–π due to the adjacent polarizing $-CF_3$ substituent.[27] Our persistent, but so far unsuccessful, attempts to crystallize **5** are consistent with a competition between nearly isoenergetic $^{\alpha}$CH–π and CF_3–π interactions. Balance **8** does not have the $^{\alpha}$CH–π option since that would cause severe steric clashes between the isopropyl R group and the ester linker (see the Supporting Information).

Given the small energy differences for **5** and **8**, and the subtle orientation variance between the computed geometry for **8** and its X-ray structure, we used the crystallographic data to determine the prevalence of such an electrostatic interaction within other known crystal structures. We performed a comprehensive Cambridge Structural Database[28] (CSD) search for aliphatic CF_3–π interactions (Chart 1), generating 2147 matches for complexes containing an aliphatic CF_3 group positioned within a 5 Å proximity of a benzenoid center. Even more noticeable is that balance **8**'s CF_3–π contact distance places it among the top 53 shortest in the entire set (all 53 have a C-to-centroid distance <4 Å). Closer inspection of the specific CF_3–π interactions in each of these 53 complexes further revealed that the CF_3 was positioned within 25° above the aromatic center in every case and that the majority (42 out of 53) had the CF_3 in an umbrella-like orientation hovering over the ring (Chart 1, inset b). The $^{\alpha}$C–$^{\beta}$C–F dihedral angle is observed just slightly reduced in **8** as the $-CF_3$ group fans

Chart 1. Comprehensive CSD Search Result for Crystals Containing the RCF_3 Group (R = C_{sp}^3) That Have the Trifluorinated C Positioned in Any Orientation within a 5 Å Sphere of the Center of a Benzenoid Ring (See Chart Inset (a))[a]

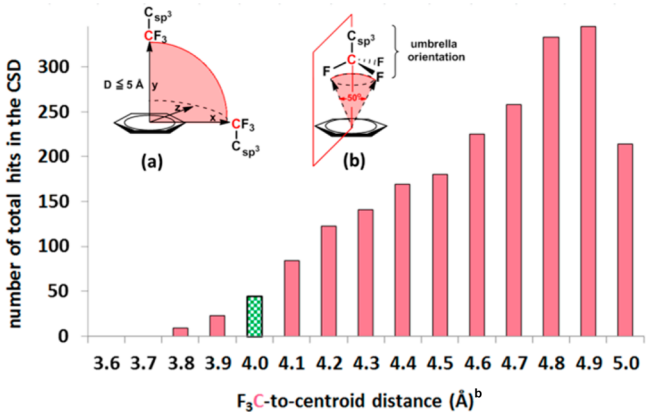

[a] Balance **8**'s short 3.968 Å CF_3–π contact distance places it among the shortest 3.5% of the 2147 total occurrences (checkered bar). Inset (b) shows the umbrella-like orientation above the benzenoid (imaginary red plane running perpendicular to the ring and running approximately through the C_{sp}^3–C bond and the Fs pointing toward benzenoid periphery). [b]Value rounded to the nearest first decimal.

DOI: 10.1021/acs.joc.5b01072
J. Org. Chem. 2015, 80, 7764−7769

upward, compared to the other $^{\alpha}C-^{\beta}CF_3$ (Figure 3) on the noninteracting portion of the ester arm. The crystal structure of the hexafluoroester derivative **8a** is provided for comparison purposes, showing two CF_3's that do not interact with π systems.

The CSD data reveal that the geometry of balance **8** is more readily explained as the consequence of the inherent balance framework than that of an electrostatic attraction. If the CF_3-benzenoid attraction was dominant, we would expect a distinct peak in the population of Chart 1 at the ∼3.9 Å distance. Rather, the fanning out of the $-CF_3$ group and its unusually short contact distance to the benzenoid center are the outcome of pushing the two groups together and maximizing the contact surface area between the tetrahedral $-CF_3$ set and the flat π surface underneath it. ^{19}F NMR data support that this is the folded conformation of **8** in $CDCl_3$ as well, a likely consequence of fluorophobic effects. In other nonfluorinated solvents such CD_2Cl_2, DMSO-d_6, and C_6D_6, the ΔG°_{fold} of **8** is virtually unchanged (−0.14, −0.11, and −0.15, respectively). Neither these solvents nor balance **8** were miscible in perfluorinated solvents, preventing our initial efforts to test for fluorophilic effects.

To summarize, our systematic study quantitatively dissects the influence of aliphatic fluorine on the CH−π attraction in solution. We found that fluorine's effect on the CH−π interplay is influential but also depends on the CH−π binding orientation. Perfluorination of the terminal end of an alkyl group tips the balance toward solvent fluorophobicity, inducing unusually close contacts with the π shelf. The observed stability trends for **1**−**8** cannot be explained as strictly electrostatic[29] but are also the result of a delicate balance occurring between conformational constraints, flexibility of the alkyl groups, and solvophobic contributions. These data can be valuable in calibrating current theoretical constructs for predicting the affinity and activity of alkyl and perfluorinated groups toward π molecular surfaces. As the fields of molecular recognition, medicinal chemistry, and materials research increasingly involve fluorine, information about these F-steering interactions provide insights into the formulation of more effective catalysts, surfactants, F-containing inhibitors, and other biomolecules.

EXPERIMENTAL SECTION

^1H, ^{19}F, and ^{13}C NMR spectra were recorded using a 400 MHz spectrometer. Flash column chromatography for benzoate ester syntheses were performed using silica gel (60 μm). Flash column chromatography for molecular balances was performed using an automated column system. All hexanes and THF were distilled. "SPhos" represents the molecule 2-dicyclohexylphosphino-2′,6′-dimethoxlbiphenyl. NMR signals abbreviations are as follows: s = singlet, d = doublet, t = triplet, q = quartet, p = pentet, and m = multiplet. In order to ensure continuity among all NMR data, all spectra were subjected to line fitting and Bernstein polynomial baseline corrections, available in MestReNova 8.0 NMR software. High-resolution mass spectra (HRMS) were recorded in the electrospray ionization (ESI) or electron impact (EI) mode on a TOF mass analyzer.

Model Procedure for Benzoate Ester Synthesis (1a−8a). Under an argon atmosphere, a flame-dried 40 mL vial (fitted with cap, septum, and stir bar) containing 2-bromo-3-methylbenzoic acid (537.6 mg, 2.5 mmol) in THF (5.0 mL) was sequentially charged with DMAP (30.5 mg, 0.25 mmol) in THF (3.0 mL, distilled) and alkyl alcohol (10.0 mmol) via syringe. DCC (515 mg, 2.5 mmol) in THF (8.0 mL, distilled) was added via syringe, and the reaction mixture was stirred for 5 min at 0 °C. The reaction mixture was then warmed to room temperature and stirred for an additional 48 h. The reaction mixture was filtered, and the remaining solution was concentrated under vacuum and isolated by silica chromatography (1:4 ethyl acetate/hexanes).

Model Procedure for Suzuki-Coupling Reaction (1−8). Under an argon atmosphere, a flame-dried 4 mL screw cap glass vial equipped with a magnetic stir bar and septum was charged with the corresponding benzoate ester (0.41 mmol), 2-methyl-8-(4,4,5,5-tetramethyl-1,3,2-dioxaborolan-2-yl)-6,12-dihydro-5,11-methanodibenzo[b,f][1,5]diazocine (150 mg, 0.41 mmol), $Pd(OAc)_2$ (4.4 mg, 0.02 mmol), and SPhos (16.3 mg, 0.04 mmol). The vial was then capped and purged with argon. Acetonitrile (0.82 mL) was added, followed by 2.0 M K_2CO_3 (0.41 mL) via syringe. The reaction mixture was stirred for 3 h at 90 °C, cooled to room temperature, and filtered through a Celite pad, eluting with ethyl acetate. The solution was washed with water and brine and dried over $MgSO_4$. The organic layer was filtered through a Celite pad, concentrated under vacuum, and isolated by silica chromatography (1:4 ethyl acetate/hexanes).

NMR and HRMS Characterization of New Compounds. *2-Fluoroethan-2-yl 2-bromo-3-methylbenzoate (**3a**):* yellow oil; yield 450 mg (70%); ^1H NMR ($CDCl_3$) δ 7.46−7.44 (m, 1H), 7.26 (m, 1H), 7.17 (m, 1H), 4.71 (td, J = 2.6 and 1.4 Hz, 1H), 4.59 (td, J = 2.6 and 1.4 Hz, 1H), 4.54 (td, J = 2.6 and 1.4 Hz, 1H), 4.47 (td, J = 2.6 and 1.4 Hz, 1H), 2.38 (s, 3H); ^{13}C NMR ($CDCl_3$) δ 166.9, 139.8, 133.5, 128.2, 127.0, 123.2, 82.1, 80.4, 64.5, 64.3, 23.8; HRMS (ESI/TOF) m/z $[M + H]^+$ calcd for $C_{10}H_{11}BrFO_2$ 260.9926, found 260.9929.

*2,2-Difluoroethan-2-yl 2-bromo-3-methylbenzoate (**4a**):* yellow oil; yield 540 mg (73%); ^1H NMR ($CDCl_3$) δ 7.49 (m, 1H), 7.32 (m, 1H), 7.20 (m, 1H), 5.93−6.21 (tt, J = 52 and 4.0 Hz, 1H), 4.49 (td, J = 16 and 4 Hz, 2H), 2.42 (s, 3H); ^{13}C NMR ($CDCl_3$) δ 166.1, 140.1, 133.9, 132.5, 128.5, 127.0, 123.5, 115.2, 112.8, 110.4, 63.6, 63.3, 63.0, 23.8; HRMS (ESI/TOF) m/z $[M + Na]^+$ calcd for $C_{10}H_9BrF_2NaO_2$ 300.9652, found 300.9658.

*2,2,2-Trifluoroethan-2-yl 2-bromo-3-methylbenzoate (**5a**):* yellow oil; yield 574 mg (77%); ^1H NMR ($CDCl_3$) δ 7.55−7.57 (m, 1H), 7.38−7.41 (m, 1H), 7.25−7.29 (m, 1H), 4.66−4.73 (q, J = 8.0 Hz, 2H), 2.46 (s, 3H); ^{13}C NMR ($CDCl_3$) δ 165.4, 140.4, 134.4, 131.9, 128.8, 127.3, 127.2, 124.6, 121.8, 119.0, 61.8, 61.4, 61.1, 60.7, 24.0; HRMS (ESI/TOF) m/z calcd for $C_{10}H_8BrF_3O_2$ 295.9657, found 295.9660.

*1,3-Difluoroisopropan-2-yl 2-bromo-3-methylbenzoate (**7a**):* yellow oil; yield 240 mg (36%); ^1H NMR ($CDCl_3$) δ 7.51−7.53 (m, 1H), 7.38−7.36 (m, 1H), 7.28−7.24 (m, 1H), 5.48 (tp, J = 20 and 4.0, 1H), 4.80−4.68 (dd, J = 48 and 4, 4H), 2.46 (s, 3H); ^{13}C NMR ($CDCl_3$) δ166.3, 140.1, 133.8, 133.8, 133.1, 128.4, 128.3, 127.1, 127.1, 81.2, 81.1, 79.5, 79.4, 79.4, 71.8, 71.6, 71.6, 23.9, 23.9; HRMS (EI/TOF) m/z calcd for $C_{11}H_{11}BrF_2O_2$ 291.99105, found 291.99062.

*1,1,1,3,3,3-Hexafluoroisopropan-2-yl 2-bromo-3-methylbenzoate (**8a**):* white solid; yield 113 mg (14%); ^1H NMR ($CDCl_3$) δ 7.63−7.61 (m, 1H), 7.48−7.46 (m, 1H), 7.34−7.33 (m, 1H), 6.00 (sept, J = 8.0 Hz, 1 H), 2.50 (s, 3H); ^{13}C NMR ($CDCl_3$) δ 163.3, 140.8, 135.1, 130.0, 129.1, 127.2, 124.8, 124.5, 122.0, 119.2, 116.4, 68.2, 67.8, 67.5, 67.2, 66.8, 66.5, 66.1, 23.9; HRMS (EI/TOF) m/z calcd for $C_{11}H_7BrF_6O_2$ 363.95334, found 363.95394; mp 52−53 °C.

*Ethyl 3-methyl-2-((11R)-8-methyl-6,12-dihydro-5,11-methanodibenzo[b,f][1,5]diazocin-2-yl)benzoate (**2**):* clear oil; yield 68 mg (35%); ^1H NMR ($CDCl_3$) δ 7.58/7.55 (d, J = 8.0 Hz, 1H), 7.35−7.30 (m, 1 H), 7.27−7.23 (m, 1H), 7.15−7.13 (m, 1 H), 7.60−6.93 (m, 1H), 6.69 (m, 2 H), 4.71−4.67 (m, 2H), 4.37−4.32 (m, 2H), 4.17−4.10 (m, 2H), 3.66−3.50/3.48−3.40 (m, 2H), 2.25/2.20 (s, 3 H), 2.13/2.04 (s, 3 H, 1.90/1.06), 0.96/0.05 (t, 3H); ^{13}C NMR ($CDCl_3$) δ 169.5, 169.1, 146.9, 146.7, 145.1, 140.7, 140.5, 137.2, 137.0, 136.3, 136.1, 133.7, 133.5, 132.9, 132.8, 132.8, 132.8, 128.3, 128.2, 128.1, 127.2, 126.9, 125.1, 124.7, 124.3, 124.3, 67.3, 67.0, 60.8, 60.6, 59.2, 59.0, 58.5, 20.9, 13.8, 12.5; HRMS (ES/TOF) m/z $[M + H]^+$ calcd for $C_{26}H_{27}N_2O_2$ 399.2073, found 399.2067.

*2-Fluoroethyl 3-methyl-2-((11R)-8-methyl-6,12-dihydro-5,11-methanodibenzo[b,f][1,5]diazocin-2-yl)benzoate (**3**):* yellow oil; yield 50 mg (30%); ^1H NMR ($CDCl_3$) δ 7.65−7.63/7.60−7.58 (d, J = 8.0 Hz, 1 H), 7.38−7.25 (m, 2 H), 7.17−6.97 (m, 4 H), 6.77−6.70

DOI: 10.1021/acs.joc.5b01072
J. Org. Chem. 2015, 80, 7764−7769

(m, 2H), 4.72−4.68 (m, 2H), 4.42−4.12 (m, 4 H), 3.76−3.64/3.63−3.51 (m, 2 H), 3.25/3.13 (m, 2H), 2.26/2.23 (s, 3 H), 2.14/2.04 (s, 3 H, 2.07/1.03); ^{13}C NMR ($CDCl_3$) δ 169.1, 168.6, 147.0, 146.8, 145.5, 145.2, 141.1, 140.9, 137.4, 137.2, 136.3, 135.9, 133.6, 133.5, 133.2, 132.0, 131.8, 128.3, 128.1, 127.8, 127.5, 127.2, 125.1, 124.9, 124.6, 124.5, 82.0, 81.0, 80.3, 79.3, 75.1, 67.3, 66.9, 63.8, 63.6, 63.4, 63.2, 59.1, 58.9, 58.5, 25.0, 20.9, 14.3; HRMS (ES/TOF) m/z $[M + H]^+$ calcd for $C_{26}H_{26}FN_2O_2$ 417.1978, found 417.1974.

*2,2-Difluoroethyl 3-methyl-2-((11R)-8-methyl-6,12-dihydro-5,11-methanodibenzo[b,f][1,5]diazocin-2-yl)benzoate (**4**):* yellow oil; yield 83 mg (50%); ^{1}H NMR ($CDCl_3$) δ 7.65−7.61 (m, 1 H), 7.40−7.28 (m, 2 H), 7.16−6.69 (m, 4 H), 6.76−6.67 (m, 2 H), 5.65−5.37 (tt, 1 H), 4.71−4.66 (m, 2 H), 4.38−4.11 (4 H), 3.72−3.61/3.55−3.44 (m, 2H, 0.76/0.66), 2.25/2.20 (s, 3 H), 2.12/2.03 (s, 3 H, 1.82/0.91); ^{13}C NMR ($CDCl_3$) δ 171.3, 168.2, 167.8, 147.0, 145.7, 145.0, 141.2, 137.5, 136.1, 134.1, 133.7, 131.0, 127.9, 127.7, 127.3, 125.2, 124.6, 114.7, 112.3, 109.9, 75.0, 67.4, 67.2, 66.9, 62.9, 62.7, 62.4, 62.1, 60.5, 59.3, 59.0, 58.5, 25.0, 20.9, 14.3; HRMS (ES/TOF) m/z $[M + H]^+$ calcd for $C_{26}H_{25}F_2N_2O_2$ 435.1884, found 435.1882.

*2,2,2-Trifluoroethyl 3-methyl-2-((11R)-8-methyl-6,12-dihydro-5,11-methanodibenzo[b,f][1,5]diazocin-2-yl)benzoate (**5**):* yellow oil; yield 64 mg (37%); ^{1}H NMR ($CDCl_3$) δ 7.66−7.64/7.58−7.56 (d, J = 8 Hz, 1H), 7.39−6.63 (m, 8 H), 4.68−4.64 (m, 2H), 4.37−4.07 (m, 4 H), 3.92−3.82/3.45−3.36 (m, 2 H), 2.24/2.18 (s, 3 H), 2.13/2.01 (s, 3 H, 3.18/2.15); ^{13}C NMR ($CDCl_3$) δ 171.3, 167.6, 167.0, 147.4, 147.2, 145.8, 145.2, 141.8, 141.4, 137.9, 137.6, 135.6, 135.4, 134.0, 133.8, 133.56, 130.8, 130.2, 128.3, 127.5, 127.3, 127.0, 125.2, 124.7, 67.4, 66.9, 60.6, 60.3, 60.0, 59.6, 59.2, 59.0, 58.6, 21.0, 20.8, 14.4; HRMS (ES/TOF) m/z $[M + H]^+$ calcd for $C_{26}H_{24}F_3N_2O_2$ 453.1790, found 453.1792.

*1,3-Difluoropropan-2-yl 3-methyl-2-((11R)-8-methyl-6,12-dihydro-5,11-ethanodibenzo[b,f][1,5]diazocin-2-yl)benzoate (**7**):* yellow oil; yield 100 mg (59%); ^{1}H NMR ($CDCl_3$) δ 7.64−7.62/7.17−7.15 (d, J = 8 Hz, 1 H), 7.40−7.27 (m, 3 H), 7.07−6.94 (m, 3 H), 6.78−6.70 (m, 2 H), 5.18−5.05/4.87−4.75 (tp, J = 20, 4.0 Hz, 1 H), 4.39−4.11 (m, 4 H), 3.70−3.32 (m, 4 H), 2.26/2.22 (s, 3 H), 2.10/2.04 (s, 3 H, 9.22/3.93); ^{13}C NMR ($CDCl_3$): δ 168.2, 147.2, 146.9, 145.4, 145.1, 141.1, 137.6, 136.4, 134.0, 133.6, 131.6, 131.3, 127.4, 125.2, 124.9, 124.7, 81.0, 80.2, 78.5, 70.1, 70.1, 69.9, 67.4, 67.0, 59.3, 59.0, 58.5, 20.9; HRMS (ES/TOF) m/z $[M + H]^+$ calcd for $C_{27}H_{27}F_2N_2O_2$ 449.2041, found 449.2041.

*1,3-Hexafluoropropan-2-yl 3-methyl-2-((11R)-8-methyl-6,12-dihydro-5,11-methanodibenzo[b,f][1,5]diazocin-2-yl)benzoate (**8**):* yellow oil; yield 73 mg (34%); ^{1}H NMR ($CDCl_3$) δ 7.73−7.71/7.67−7.65 (d, J = 8.0 Hz, 1 H), 7.47−6.66 (m, 8 H), 5.76/5.50 (sept, J = 8.0 Hz, 1 H), 4.73−4.64 (m, 2 H), 4.39−4.07 (m, 4 H), 2.26/2.22 (s, 3 H), 2.08/2.04 (s, 3 H, 0.94/0.79); ^{13}C NMR ($CDCl_3$) δ 183.4, 165.8, 165.0, 147.9, 147.4, 145.1, 144.7, 142.3, 141.7, 138.4, 138.3, 135.1, 134.9, 133.9, 133.8, 133.67, 128.6, 128.4, 128.4, 128.3, 128.0, 127.9, 127.8, 127.7, 127.4, 127.4, 127.3, 127.1, 125.1, 124.9, 124.2, 67.0, 58.7, 21.0, 20.9, 20.8; HRMS (ES/TOF) m/z $[M + H]^+$ calcd for $C_{27}H_{23}F_6N_2O_2$ 521.1664, found 521.1658.

Model Procedure for Quantification of Folded/Unfolded Conformers in Solution. The ratio of folded to unfolded conformation for each balance was determined by the integration of both the top methyl singlets in the ^{1}H NMR spectra. Due to the anisotropic effect, the furthest upfield peak represents the unfolded top methyl hydrogens. This is paired with the next closest upfield peak (based on integration and temperature dependent NMR analysis). The methyl peaks for the folded and unfolded conformations can be used to determine the Gibbs free energy using the equation $\Delta G^\circ_{folded} = -RT \ln(K_{folded}) = -RT \ln(\text{folded/unfolded})$. The ratio of folded to unfolded conformation for balance **8** was confirmed by ^{19}F NMR in $CDCl_3$, CD_2Cl_2, DMSO-d_6, and C_6D_6. The folded conformation shows two signals for the chemically inequivalent $-CF_3$ groups and one signal representing both $-CF_3$ groups for the unfolded conformation. All NMR spectra have corrected baselines and were fitted to a Gaussian (line fitting/deconvolution) function using MNova 8 NMR software.

■ ASSOCIATED CONTENT

Supporting Information

^{1}H and ^{13}C NMR spectra for all newly reported compounds, error analysis, NMR spectroscopy experiments, computational details, and X-ray data for **1**−**4**, **6**−**8**, and **8a** (CIF). The Supporting Information is available free of charge on the ACS Publications website at DOI: 10.1021/acs.joc.5b01072.

■ AUTHOR INFORMATION

Corresponding Author

*E-mail: mams@allegheny.edu.

Notes

[‖](M.F., T.G., R.S., A.S.) Undergraduate student at Allegheny College.

The authors declare no competing financial interest.

■ ACKNOWLEDGMENTS

The research was supported by an award from Research Corporation for Scientific Advancement, The Thomas Lord Charitable Trust Fellowship, and Allegheny College. The X-ray diffractometer was funded by NSF Grant Nos. 0087210 and 1337296, Ohio Board of Regents Grant No. CAP-491, and by Youngstown State University. We are grateful for helpful discussions with Dr. Brijesh Bhayana (Massachusetts General Hospital), S. Shaun Murphree (Allegheny College), and Agustí Lledó-Ponsatí (University of Girona) and insight provided by Dr. Allen D. Hunter (Youngstown State University).

■ REFERENCES

(1) Scholfield, M. R.; Zanden, C. M. V.; Carter, M.; Ho, S. *Protein Sci.* **2013**, *22*, 139−152.

(2) Johnson, E. R.; Keinan, S.; Mori-Sanchez, P.; Contreras-Garcia, J.; Cohen, A. J.; Yang, W. *J. Am. Chem. Soc.* **2010**, *132*, 6498−6506.

(3) (a) Umezawa, Y.; Tsuboyama, S.; Takahashi, H.; Uzawa, J.; Nishio, M. *Tetrahedron* **1999**, *55*, 10047−10056. (b) Bazzicalupi, C.; Dapporto, P. *Struct. Chem.* **2004**, *15*, 259−268. (c) Singh, N. J.; Min, S. K.; Kim, D. Y.; Kim, K. S. *J. Chem. Theory Comput.* **2009**, *5*, 515−529. (d) Vacas, T.; Corzana, F.; Jimenez-Oses, G.; Gonzalez, C.; Gomez, A. M.; Bastida, A.; Revuelta, J.; Asensio, J. L. *J. Am. Chem. Soc.* **2010**, *132*, 12074−12090. (e) Ozawa, T.; Okazaki, K.; Kitaura, K. *J. Comput. Chem.* **2011**, *32*, 2774−2782. (f) Asensio, J. L.; Arda, A.; Canada, F. J.; Jimenez, -Barbero *Acc. Chem. Res.* **2013**, *46*, 946−954.

(4) (a) Nishio, M.; Hirota, M. *Tetrahedron* **1989**, *45*, 7201. (b) Nishio, M.; Umezawa, Y.; Hirota, M.; Takeuchi, Y. *Tetrahedron* **1995**, *51*, 8665. (c) Tewari, A. K.; Dubey, R. *Bioorg. Med. Chem.* **2008**, *16*, 126. (d) Nishio, M.; Umezawa, Y.; Honda, K.; Tsuboyama, S.; Suezawa, H. *CrystEngComm* **2009**, *11*, 1757. (e) Takahashi, O.; Kohno, Y.; Nishio, M. *Chem. Rev.* **2010**, *110*, 6049. (f) Nishio, M. *Phys. Chem. Chem. Phys.* **2011**, *13*, 13873. (g) Zhang, Z. B.; Xia, B. Y.; Han, C. Y.; Yu, Y. H.; Huang, F. H. *Org. Lett.* **2010**, *12*, 3285. (h) Zhang, Z. B.; Yu, G. C.; Han, C. Y.; Liu, J. Y.; Ding, X.; Yu, Y. H.; Huang, F. H. *Org. Lett.* **2011**, *13*, 4818. (i) Xue, M.; Yang, Y.; Chi, X. D.; Zhang, Z. B.; Huang, F. H. *Acc. Chem. Res.* **2012**, *45*, 1294.

(5) (a) Chopra, D. *Cryst. Growth Des.* **2012**, *12*, 541−546. (b) Walker, M. C.; Thuronyi, B. W.; Charkoudian, L. K.; Lowry, B.; Khosla, C.; Chang, M. C. Y. *Science* **2013**, *341*, 1089−1094.

(6) Jackel, C.; Koksch, B. *Eur. J. Org. Chem.* **2005**, *2005*, 4483−4503.

(7) Jackel, C.; Salwiczek, M.; Koksch, B. *Angew. Chem., Int. Ed.* **2006**, *45*, 4198−4203.

(8) (a) Nakagawa, Y.; Irie, K.; Yanagita, R. C.; Ohigashi, H.; Tsuda, K. *J. Am. Chem. Soc.* **2005**, *127*, 5746−5747. (b) Leimbacher, M.; Zhang, Y.; Mannocci, L.; Stravs, M.; Geppert, T.; Scheuermann, J.; Schneider, G.; Neri, D. *Chem. - Eur. J.* **2012**, *18*, 7729−7737.

(9) For articles discussing crystal data in the Cambridge Structural Databank and the Protein Data Bank for F in close proximity to π

DOI: 10.1021/acs.joc.5b01072
J. Org. Chem. 2015, 80, 7764−7769

systems, see: (a) Matter, H.; Nazare, M.; Gussregen, S.; Will, D. W.; Schreuder, H.; Bauer, A. *Angew. Chem., Int. Ed.* **2009**, *49*, 2911. (b) Bissantz, C.; Kuhn, M.; Stahl, M. *J. Med. Chem.* **2010**, *53*, 5061. (c) Sun, H. *Cryst. Growth Des.* **2012**, *12*, 5655−5662. (d) Chopra, D. *Cryst. Growth Des.* **2012**, *12*, 541−546.

(10) (a) Muller, K.; Faeh, C.; Diederich, F. *Science* **2007**, *317*, 1881−1886. (b) Fernandez, A.; Fraser, C.; Scott, L. R. *Trends Biotechnol.* **2012**, *30*, 1−7. (c) Vulpetti, A.; Dalvit, C. *Drug Discovery Today* **2012**, *17*, 890−897.

(11) (a) Kim, E.; Paliwal, S.; Wilcox, C. S. *J. Am. Chem. Soc.* **1998**, *120*, 11192−11193. (b) DerHovanessian, A.; Rablen, P. R.; Jain, A. *J. Phys. Chem. A* **2000**, *104*, 6056−6061. (c) Gardarsson, H.; Schweizer, W. B.; Trapp, N.; Diederich, F. *Chem. - Eur. J.* **2014**, *20*, 4608−4616. (d) Garcia, A. M.; Determan, J. J.; Janesko, B. G. *J. Phys. Chem. A* **2014**, *118*, 3344−3350.

(12) (a) Saraogi, I.; Vijay, V. G.; Das, S.; Sekar, K.; Guru Row, T. N. *Cryst. Eng.* **2003**, *6*, 69−77. (b) Jackel, C.; Salwiczek, M.; Koksch, B. *Angew. Chem., Int. Ed.* **2006**, *45*, 4198−4203.

(13) Two related experimental studies reporting some aspects of alkyl F−π strengths are have been published but contain notable limitations: (a) Adams, H.; Cockroft, S. L.; Guardigli, C.; Hunter, C. A.; Lawson, K. R.; Perkins, J.; Spey, S. E.; Urch, C. J.; Ford, R. *ChemBioChem* **2004**, *5*, 657−665. The model system in this study is limited by solubility issues, complexation, competing steric/electrostatic effects, and the geometry of the system. (b) Thomas, K. M.; Naduthambi, D.; Zondlo, N. J. *J. Am. Chem. Soc.* **2006**, *128*, 2216−2217 The model system in this study does not strictly isolate the CH−π interaction..

(14) (a) Ismail, F. M. D. *J. Fluorine Chem.* **2002**, *118*, 27−33. (b) Reference 8. (c) Purser, S.; Moore, P. R.; Swallow, S.; Gouverneur, V. *Chem. Soc. Rev.* **2008**, *37*, 320−330. (d) Fabbri, L. M.; Calverley, P. M. A.; Izquierdo-Alonso, J. L.; Bundschuh, D. S.; Brose, M.; Martinez, F. J.; Rabe, K. F. *Lancet* **2009**, *374*, 695−703.

(15) For several recent advances in the synthesis of aliphatic fluorine compounds, see: (a) Ritter, T. *Nature* **2010**, *466*, 447−448. (b) Furuya, T.; Kamlet, A.; Ritter, T. *Nature* **2011**, *473*, 470−477. (c) Reference 5b.

(16) Lu, Y.; Wang, Y.; Zhu, W. *Phys. Chem. Chem. Phys.* **2010**, *12*, 4543−4551.

(17) (a) Raju, R. K.; Bloom, J. W.; An, Y.; Wheeler, S. E. *ChemPhysChem* **2011**, *12*, 3116−3130. (b) Raju, R. K.; Bloom, J. W. G.; An, Y.; Wheeler, S. E. *ChemPhysChem* **2011**, *12*, 3116−3130.

(18) (a) Paliwal, S.; Geib, S.; Wilcox, C. S. *J. Am. Chem. Soc.* **1994**, *116*, 4497−4498. (b) Kim, E.; Paliwal, S.; Wilcox, C. S. *J. Am. Chem. Soc.* **1998**, *120*, 11192−11193. (c) Hof, F.; Scofield, D. M.; Schweizer, W. B.; Diederich, F. *Angew. Chem., Int. Ed.* **2004**, *43*, 5056−5059. (d) Fischer, F. R.; Schweizer, W. B.; Diederich, F. *Chem. Commun.* **2008**, 4031−4033. (e) Bhayana, B.; Ams, M. R. *J. Org. Chem.* **2011**, *76*, 3594−3596. (f) Bhayana, B. *J. Org. Chem.* **2013**, *78*, 6758−6762. (g) Yang, L.; Adam, C.; Nichol, G.; Cockroft, S. L. *Nat. Chem.* **2013**, *5*, 1006−1010. (h) Gardarsson, H.; Schweizer, W. B.; Trapp, N.; Diederich, F. *Chem. - Eur. J.* **2014**, *20*, 4608−4616.

(19) (a) Carroll, W. R.; Pellechia, P.; Shimizu, K. D. *Org. Lett.* **2008**, *10* (16), 3547−3550. (b) Carroll, W. R.; Zhao, C.; Smith, M. D.; Pellechia, P. J.; Shimizu, K. D. *Org. Lett.* **2011**, *13* (16), 4320−4323. (c) Zhao, C.; Parrish, R. M.; Smith, M. D.; Pellechia, P. J.; Sherrill, C. D.; Shimizu, K. D. *J. Am. Chem. Soc.* **2012**, *134* (35), 14306−14309. (d) Li, P.; Zhao, C.; Smith, M. D.; Shimizu, K. D. *J. Org. Chem.* **2013**, *78* (11), 5303−5313. (e) Zhao, C.; Smith, M. D.; Pellechia, P. J.; Shimizu, K. D. *Org. Lett.* **2014**, *16*, 3520−3523.

(20) (a) A explanation of how the folding ratios are quantified by ^{1}H NMR is provided in the Supporting Information, along with NMR spectra, coalescence NMR experiments, and details of the DFT calculations.. (b) The crystal structure of **7** contained two different folded conformers with slightly different geometries, each showing CH−π interactions. Only one congener of **7** is shown in the manuscript..

(21) (a) Tsuzuki, S.; Honda, K.; Uchimaru, T.; Mikami, M.; Fujii, A. *J. Phys. Chem. A* **2006**, *110*, 10163−10168. Unlike the heavier halogens, fluorine is too polarized to contain a σ hole and repels π clouds. For further references, see: (b) Forni, A.; Pieraccini, S.; Rendine, S.; Sironi, M. *J. Comput. Chem.* **2014**, *35*, 386−394. (c) Lu, Y.; Zou, J.; Wang, Y.; Yu, Q. *Chem. Phys.* **2007**, *334*, 1−7.

(22) (a) Tsuzuki, S.; Honda, K.; Uchimaru, T.; Mikami, M.; Tanabe, K. *J. Am. Chem. Soc.* **2000**, *122*, 3746−3753. (b) Tsuzuki, S.; Honda, K.; Uchimaru, T.; Mikami, M.; Tanabe, K. *J. Phys. Chem. A* **2002**, *106*, 4423−4428.

(23) To illustrate the known influence of fluorination on the CH−π interaction, we performed DFT-D and coupled cluster calculations for gas-phase interaction energies between benzene and CH_4, CH_3F, CH_2F_2, CHF_3, and CF_4 (see the Supporting Information). They reproduce fluorination's known large effect on CH−π interactions in gas-phase benzene−CH_nF_{4-n} complexes. The coupled cluster binding energies are −1.44, −2.49, −3.40, −4.24, and −1.89 kcal/mol, respectively. The differences between these gas-phase interactions and those seen for the balances are consistent with the fact that the methane derivatives bind with an optimal orientation, while the R groups under consideration are constrained by the structure of the balance's scaffold.

(24) (a) Vangala, V. R.; Nangia, A.; Lynch, V. M. *Chem. Commun.* **2002**, 1304−1305. (b) DerHovanessian, A.; Doyon, J. B.; Jain, A.; Rablen, P. R.; Sapse, A. *Org. Lett.* **1999**, *1* (9), 1359−1362. (c) Reimann, B.; Buchhold, K.; Vaupel, S.; Brutschy, B.; Havlas, Z.; Spirko, V.; Hobza, P. *J. Phys. Chem. A* **2001**, *105*, 5560−5566. (d) Neretin, I. S.; Lyssenko, K. A.; Antipin, M. Y.; Slovokhotov, Y. L.; Boltalina, O. V.; Troshin, P. A.; Lukonin, A. Y.; Sidorov, L. N.; Taylor, R. *Angew. Chem.* **2000**, *112*, 3411−3414.

(25) Wheeler, S. E.; Houk, K. N. *J. Am. Chem. Soc.* **2008**, *130*, 10854−10855.

(26) DFT-D calculations on balances **1**−**8** in continuum chloroform solvent, starting from the experimental crystal structures, give computed ΔE_{fold} values of −1.51 (**1**), −2.16 (**2**), −1.98 (**3**), −1.21 (**4**), −2.70 (**5**), −2.66 (**6**), −3.27 (**7**), and −1.99 (**8**). Consistent with the experimentally obtained ΔG°_{fold} values, **7** and **8** have ΔE_{fold} values more and less negative (respectively) than balance **6**. Balance **7** has the most negative overall ΔE_{fold} value, and **1** has ΔE_{fold} less negative than **2**. The predicted effect of fluorination on balances **2**−**4** is reduced or even reversed relative to the benzene−CH_nF_{4-n} complexes in ref 23. The computed ΔE_{fold} thus seem to capture or overestimate the conformational effects discussed in ref 23. Overall, the folding of balances **2**−**4** appears to involve a subtle interplay of electrostatic attraction, steric constraints, and other effects (solvophobic, entropic, etc.) that are not captured by DFT-D calculations on single conformations. As in our previous work, these effects make the computed ΔE_{fold} values substantially more negative than experimental ΔG°_{fold} values. See: Janesko, B. G.; Ams, M. R. *Theor. Chem. Acc.* **2014**, *133*, 1490.

(27) Several theoretical studies have been conducted on the effects of fluorine and the CH−π interaction. For more information, we direct the reader to: (a) Menapace, J. A.; Bernstein, E. R. *J. Phys. Chem.* **1987**, *91*, 2843−2848. (b) Reference 22b. (c) Kawahara, S.; Tsuzuki, S.; Uchimaru, T. *J. Phys. Chem. A* **2004**, *108*, 6744−6749. (d) Reference 21. (e) Lu, Y.; Zou, J.; Wang, Y.; Yu, Q. *Chem. Phys.* **2007**, *334*, 1−7. (f) Dey, R. C.; Seal, P.; Chakrabarti, S. *J. Phys. Chem. A* **2009**, *113*, 10113−10118.

(28) Groom, C. R.; Allen, F. H. *Angew. Chem., Int. Ed.* **2014**, *53*, 662−671.

(29) The Supporting Information shows the molecular electrostatic potential computed for R groups **1**−**8**. Hunter's model for hydrogen bonding interactions predicts a linear dependency for the electrostatic minima of these and ΔG°_{fold}, but in agreement with the Diederich laboratory, we do not observe a close correlation. For details of Hunter's model, see: (a) Hunter, C. A. *Angew. Chem., Int. Ed.* **2004**, *43*, 5310−5324. (b) Cockroft, S. L.; Hunter, C. A. *Chem. Commun.* **2006**, 3806−3808. (c) Cockroft, S. L.; Hunter, C. *Chem. Commun.* **2009**, 3961−3963. For the Diederich studies, see: (d) Gardarsson, H.; Schweizer, W. B.; Trapp, N.; Diederich, F. *Chem. - Eur. J.* **2014**, *20*, 4608−4616.

DOI: 10.1021/acs.joc.5b01072
J. Org. Chem. 2015, 80, 7764−7769